

Figure 1. Resonance Raman spectra of **1**, **2**, and **3** at $\sim 0^\circ\text{C}$ and 6764-Å laser excitation. **1** was 12 mM Pt, prepared from *cis*-diammineplatinum α -pyridone blue in 0.05 M HNO_3 . **2** was 12 mM Pt, prepared from *cis*-diammineplatinum 1-methyluracil blue in H_2O . **3** was 12 mM Pt, prepared from (ethylenediamine)platinum α -pyridone blue in 0.10 M HNO_3 . Inset: Resonance Raman spectrum ($40\text{--}1700\text{ cm}^{-1}$) of **1** at $\sim 0^\circ\text{C}$ and 6764-Å laser excitation. **1** was 12 mM Pt, prepared from *cis*-diammineplatinum α -pyridone blue in 0.05 M HNO_3 and 0.24 M NaN_3O_3 .

Table I. Comparison of the Optical Transitions, Pt-Pt Vibrational Frequencies, and Pt-Pt Distances of Three Pt_4^{9+} Cations

compd	$\nu(\text{Pt-Pt})^a$ cm^{-1}	optical bands, ^b nm	Pt-Pt dist, ^c Å	ref
1	149, 69	480, 680	2.774, 2.877, 2.774	4, 14, 20
2	149, 67	480, 740	2.793, 2.865, 2.810	5, 2c
3	133, 67	532, 745	2.830, 2.906, 2.830	6

^aThis work. ^bThe extinction coefficients are roughly 250 and 8000 $\text{M}^{-1}\text{ cm}^{-1}$, respectively.^{2c} ^cThe second entry is the Pt2-Pt2' distance.

$\nu(\text{Pt2-Pt2}') = 84\text{ cm}^{-1}$ and $\nu(\text{Pt1-Pt2}) = 164\text{ cm}^{-1}$ and Pt1-Pt2 = 2.704 Å and Pt2-Pt2' = 2.710 Å.^{2b}

With 6764-Å laser excitation, the rR spectrum of **1** (see insert in Figure 1) displays *only* bands due to the Pt-Pt stretching vibrations and certifies that the intense optical absorption at 680 nm¹⁴ is assigned to a metal-metal transition.¹⁸ According to the SCF-X α -SW calculation of **1**, the optical transition is given as a $\sigma(\text{Pt2-Pt2}') \rightarrow \sigma^*(\text{Pt2-Pt2}')$ with some Pt1 \rightarrow Pt2 charge-transfer character.¹⁹ Raman depolarization ratios of one-third support a z-polarized electronic transition. The weak optical absorption at 480 nm in **1** is assigned to a $\pi(\text{Pt1-Pt2}) \rightarrow \sigma^*(\text{Pt1-Pt2})$ transition.¹⁹ Absorption maximum, Pt-Pt distances, and $\nu(\text{Pt-Pt})$ for **1**, **2**, and **3** are given in Table I and their low-frequency rR spectra are shown in Figure 1.

The Pt-Pt stretching frequencies are used as sensitive indicators to explain the variations in the absorption maxima of **1**, **2**, and **3**. Although the changes in $\nu(\text{Pt2-Pt2}')$ are numerically small (2-3 cm^{-1}), they indicate a stronger Pt2-Pt2' interaction in **1** relative to **2** or **3** and correlate well with the observed shifts of the intense optical absorption. The N-H \cdots O interdimer hydrogen bonds stabilize the Pt_4^{9+} complexes and contribute to $\nu(\text{Pt2-Pt2}')$. Differences in N-H \cdots O bonding may result from the steric re-

(17) Stein, P.; Mahtani, H. K. *Proc. Xth Int. Conf. Raman Spectrosc.*; Peticolas, W. L., Hudson, B., Eds.; University of Oregon Press: Eugene, 1986; Chapter 13, pp 8-9.

(18) Spiro, T. G.; Stein, P. *Annu. Rev. Phys. Chem.* **1977**, *28*, 501.

(19) Ginsberg, A. P.; O'Halloran, T. V.; Fanwick, P. E.; Hollis, L. S.; Lippard, S. J. *J. Am. Chem. Soc.* **1984**, *106*, 5430.

(20) Laurent, M. P.; Tewksbury, J. C.; Krogh-Jespersen, M.-B. *Inorg. Chem.* **1980**, *19*, 1656.

(21) The sample of **2** reported here has an absorption spectrum similar to the one given in ref 2c. An additional weak absorption band at 520 nm, previously reported for **2**,⁵ has also been observed by us during these studies. The rR spectra of these samples will be presented elsewhere along with rR spectra of certain platinum pyrimidine blues. Typically, the Pt_4^{9+} cations show instability in solution, and the presence of absorption bands due to decomposition and oligomerization products may occur.

quirements of the en ligands and electron density of the exocyclic oxygens. $\nu(\text{Pt1-Pt2})$ indicates a weaker Pt1-Pt2 interaction in **3** relative to **1** or **2** and nicely correlates with the red shift of the weak optical transition observed for **3**. Nonbonding repulsions of en in adjacent coordination planes attenuate the Pt1-Pt2 bond strength in **3**.²² The variations in the peak positions of the absorption bands originate from localized interactions of the coordinating ligands along the Pt_4^{9+} chain. The vibrational data demonstrate that the intense optical absorption is primarily sensitive to changes of the interdimer interactions and the weak optical absorption is primarily sensitive to changes of the intradimer Pt1-Pt2 interactions. These results are consistent with and provide support for the assignments of the optical transitions.

The crystallographic measurements of the Pt-Pt distances, as given in Table I, are compatible with the present discussion of **1** and **3**; however, the Pt-Pt distances of **2** are at variance with the analysis of the optical transitions and the rR data. It should not be surprising that structural changes occur in these interesting tetranuclear platinum complexes upon dissolution because of the feeble Pt2-Pt2' interactions. Solid-state absorption data of **2** and **3** have not been reported to our knowledge, while differences in **1** have been observed.^{19,20} Since the rR and absorption data were obtained under the same solution conditions, and present analysis is not obfuscated by this lacuna.

Acknowledgment. Support from the National Science Foundation (Grant CHE-8307651) is gratefully acknowledged. This work was also supported by a grant from the Research Corp.

(22) For example, the Pt_2^{III} dimer, $[\text{Pt}_2(\text{en})_2(\text{C}_5\text{H}_5\text{NO})_2(\text{NO}_2)(\text{NO}_3)] \cdot 0.5\text{H}_2\text{O}$, has a Pt-Pt bond distance of 2.64 Å (see: O'Halloran, T. V.; Roberts, M. M.; Lippard, S. J. *Inorg. Chem.* **1986**, *25*, 957) and $\nu(\text{Pt-Pt}) = 164\text{ cm}^{-1}$.

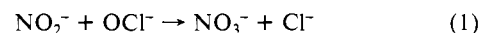
Reactions between Metal Carbonyl Anions and Cations: Rapid Two-Electron Transfer Followed by One-Electron Back Transfer

Yueqian Zhen and Jim D. Atwood*

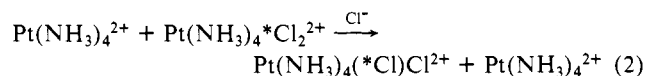
Department of Chemistry, University at Buffalo
State University of New York
Buffalo, New York 14214

Received October 18, 1988

Definitive examples of single-event, two-electron transfer are relatively rare. Examples of oxide transfer



and a few examples of transition-metal complexes



have been reported as two-electron transfers.¹⁻³ We now report, as part of our continuing study of electron-transfer reactions between organometallic complexes,⁴ that reaction of $\text{Re}(\text{CO})_5^-$ with $\text{Mn}(\text{CO})_6^+$ proceeds by a rapid two-electron, one-carbonyl transfer and then a slower one-electron back transfer to the binuclear products. Self-exchange between $\text{M}(\text{CO})_5^-$ and $\text{M}(\text{CO})_6^+$ ($\text{M} = \text{Mn, Re}$) in acetonitrile occurs by the same steps.

(1) Halpern, J. *Quart. Rev.* **1961**, *15*, 207.

(2) Sykes, A. G. *Adv. Inorg. Chem. Radiochem.* **1967**, *10*, 153.

(3) Taube, H. *Electron Transfer Reactions of Complex Ions in Solution*; Academic Press: New York, 1970.

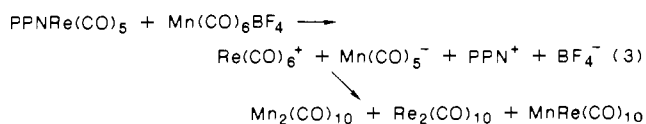
(4) Atwood, J. D. *Inorg. Chem.* **1987**, *26*, 2918.

Table I. Infrared Spectra of Manganese and Rhenium Cations and Anions

compound	solvent ^a	IR ^b
PPNMn(CO) ₅	a	1825 (sh), 1861 (br, vs), 1892 (s)
	b	1829 (sh), 1864 (br, vs), 1902 (s)
	c	1850 (br), 1895
PPNRe(CO) ₅	a	1828 (sh), 1862 (br, vs), 1907 (s)
	b	1829 (sh), 1864 (br, vs), 1918 (s)
	c	1850 (br), 1910 (s)
Mn(CO) ₆ BF ₄	b	2062 (sh), 2096 (sharp, s)
	c	2060 (sh), 2086 (sharp, s)
Re(CO) ₆ BF ₄	b	2050 (sh), 2083 (sharp, s)
	c	2040 (sh), 2078 (sharp, s)
Re(¹³ CO) ₆ BF ₄	b	2039, 2051, 2084
Mn(¹³ CO) ₆ BF ₄	b	2050, 2062, 2096

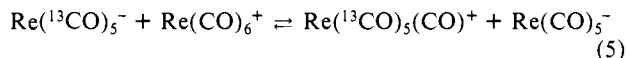
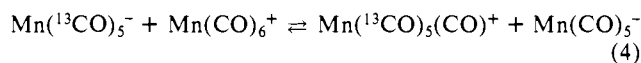
^aSolvents: a = THF, b = CH₃CN, c = CH₃COCH₃. ^bAll infrared spectra were recorded on a Beckman 4240 spectrophotometer.

When PPNRe(CO)₅⁻ and Mn(CO)₆BF₄⁺ are mixed,⁷ the infrared spectrum shows immediate, quantitative formation of Re(CO)₆⁺ and Mn(CO)₅⁻ (all infrared spectra are reported in Table I). Over the next 2 h, the infrared spectra indicate the formation of binuclear complexes (Mn₂(CO)₁₀, Re₂(CO)₁₀, and MnRe(CO)₁₀); the exact ratios depend strongly on the relative initial amounts of cation and anion. The same three binuclear



products are obtained by reacting Re(CO)₆⁺ with Mn(CO)₅⁻, though in different ratios. The binuclear products were isolated, separated, and identified by their infrared spectra.⁸

As previously noted, reaction of Mn(CO)₅⁻ with Mn(CO)₆⁺ gives Mn₂(CO)₁₀ and reaction of Re(CO)₅⁻ with Re(CO)₆⁺ gives Re₂(CO)₁₀.^{9,10} Use of ¹³CO labeled anions shows that both of these reactions are accompanied by a rapid two-electron transfer.¹²



(5) Re₂(CO)₁₀ (2.0 g) in 20 mL of ethyl ether and 2 mL of CH₃CN was first stirred with 10 mL of 1% Na(Hg) amalgam in the inert atmosphere glovebox for 10 h and the yellow solution was separated and dried under reduced pressure. PPNCl (3.5 g) in 10 mL of CH₃CN was then added and stirred for another 20 min. The yellow cloudy solution was dried again by vacuum, and then 30 mL of THF was added to extract the product. After filtering the orange THF solution with Celite filter aid, the volume was reduced to 10 mL, and ether was added to crystallize the orange salt. The yield is quantitative.

(6) Beach, N. A.; Gray, H. B. *J. Am. Chem. Soc.* **1968**, *90*, 5713.

(7) For a typical reaction, equal amounts of the two reactants (10–30 mg) were mixed in the inert atmosphere glovebox and 15 mL of CH₃CN was then added to the mixture. The infrared spectrum in CH₃CN was recorded immediately on a Beckman 4240 spectrophotometer and was monitored every 20 min.

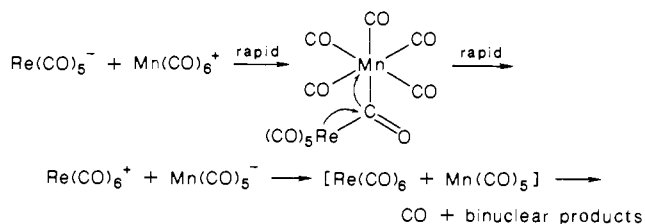
(8) After completion, the solvent was removed by vacuum, and the solid was extracted with hexanes to separate the dimers from remaining ionic species. The hexanes solution was concentrated, and the dimers were separated on an alumina column.

(9) Lee, K. Y.; Kuchynka, D. J.; Kochi, J. K. *Organometallics* **1987**, *6*, 1886.

(10) In acetonitrile, the reaction of Mn(CO)₅⁻ with Mn(CO)₆⁺ also gives Mn₂(CO)₉(NCCH₃).¹¹

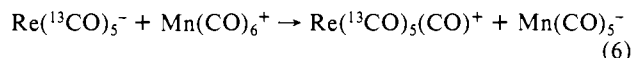
(11) Koelle, U. *J. Organomet. Chem.* **1978**, *155*, 53.

(12) Enrichment levels of the cations and anions were typically around 70%. Mn(CO)₆⁺, at that level of enrichment, has two carbonyl stretches at 2050 and 2062 in addition to that for unenriched at 2095 cm⁻¹. The 2050-cm⁻¹ absorbance dominates at high enrichment. In reaction 4, within 5 min of mixing, peak 2062 is only a shoulder; at 10 min, the two peaks become equal; within 20 min, peak 2050 becomes a shoulder. Thus the initial high enrichment from the presence of Mn(¹³CO)₅(CO)⁺ is decreased in 20 min. For Re(CO)₆⁺ the situation is similar with infrared absorptions at 2039 and 2050 cm⁻¹ in addition to 2083 cm⁻¹. For reaction 5, within 5 min, one observes two ¹³CO peaks: 2039 (a shoulder) and 2050 (strong). Thus the rhenium exchange has already come to the equilibrium enrichment.

Scheme I^a

^aProposed scheme for the reaction of Re(CO)₅⁻ with Mn(CO)₆⁺ involving an initial rapid two-electron transfer followed by a slower back transfer of one electron.

Reactions 4 and 5 must be sampled early in the reaction before complete scrambling of the label occurs. The dimers invariably had ¹³CO completely scrambled, as expected for a reaction proceeding through the odd-electron species, M(CO)₅ and M(CO)₆. Reaction 4 reached equilibrium in 25 min; formation of Mn₂(C-O)₁₀ had a half-life of 3 h. Reaction 5 reached equilibrium in 10 s; formation of Re₂(CO)₁₀ occurred with a half-life of 20 min. Similar transfer of one labeled CO is seen for reaction of enriched Re(¹³CO)₅⁻ with Mn(CO)₆⁺.¹² The reverse of reaction 6 did not

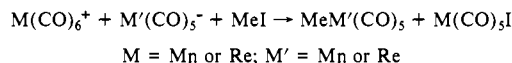


occur; Re(CO)₆⁺ did not transfer a CO to Mn(¹³CO)₅⁻, although, in this case, the binuclear products also have ¹³CO scrambled throughout. If reaction 3 is run under an atmosphere of ¹³CO, no incorporation of ¹³CO into Re(CO)₆⁺ or Mn(CO)₅⁻ is observed.

Reactions 3, 4, and 5 provide clear examples of single-event, two-electron transfer. The cationic products have been characterized by infrared spectra and, through reaction with MeI, by mass spectroscopy.¹³ A single-electron transfer would lead to the odd-electron species M(CO)₅ and M(CO)₆ which are known to rapidly dimerize and to undergo ligand exchange.¹⁴ We do not observe either on the time scale of the two-electron transfer. The scheme in Figure 1 summarizes our interpretation of reaction 3. First the nucleophile Re(CO)₅⁻ attacks a carbon of Mn(CO)₆⁺. It is unclear whether the bridged intermediate has a finite lifetime. The bridging carbonyl–manganese bond is heterolytically split with the manganese retaining the electron pair. Thus, formally, a CO²⁺ is transferred from Mn(CO)₆⁺ to Re(CO)₅⁻. This can be viewed as a nucleophilic attack (Re(CO)₅⁻) resulting in displacement of a weaker nucleophile (Mn(CO)₅⁻). At this point we cannot distinguish between an outer sphere and a nucleophilic attack mechanism for the subsequent single-electron transfer resulting in the odd-electron complexes. An inner sphere mechanism requiring CO loss from M(CO)₅⁻ or M(CO)₆⁺ can be eliminated because the cations and anions are inert toward exchange or substitution.¹⁵

A similar scheme apparently holds for reactions 3–6 and nicely accounts for the product distribution. In reaction 3, when an excess of Re(CO)₆⁺ is used, Re₂(CO)₁₀ dominates as dimeric product

(13) We have found the reaction of MeI with the cations and anions to be useful in characterizing the level of enrichment by mass spectroscopy.



This reaction takes place in two steps with the metal carbonyl anion reacting with MeI to generate MeM'(CO)₅ and I⁻. The cation reacts with I⁻ to give M(CO)₅I. In the absence of the metal carbonyl anion no reaction is observed between M(CO)₆⁺ and MeI. Both MeM'(CO)₅ and M(CO)₅I are sufficiently volatile for excellent mass spectra. Reaction of unlabeled metal carbonyl cation and anion with MeI in the presence of ¹³CO gives no incorporation of ¹³CO into MeM'(CO)₅ or M(CO)₅I so that the labeling in MeM'(CO)₅ and M(CO)₅I accurately represent the labeling in the metal carbonyl anion and cation. In a typical reaction the two reactants were mixed in equal amounts in a pressure tube and CH₃CN was introduced through the vacuum line. After stirring, the reaction was stopped by liquid N₂, and MeI was introduced. A mass spectrum was taken after the solution was stirred for 30 min. In reaction 4, the mass spectrum showed formation of Mn(CO)₅I at 322, 323, and 324; for reaction 5, the mass spectrum showed formation of Re(CO)₅I at 452–463.

(14) Stiegman, A. E.; Tyler, D. R. *Comments Inorg. Chem.* **1986**, *5*, 215.

(15) Angelici, R. J. *Organomet. Chem. Rev.* **1968**, *3*, 173.

because of the very rapid single-electron-transfer reaction between $\text{Re}(\text{CO})_6^+$ and $\text{Re}(\text{CO})_5^-$ in comparison to the single-electron transfer of $\text{Re}(\text{CO})_6^+$ and $\text{Mn}(\text{CO})_5^-$ ($t_{1/2} = 8$ h). Reaction 3 yields very little (<10%) of the mixed-metal product. In contrast, reaction between $\text{Re}(\text{CO})_6^+$ and $\text{Mn}(\text{CO})_5^-$ provides yields of $\text{MnRe}(\text{CO})_{10}$ up to 50%.

In this communication, we have reported the first example of two-electron transfer to a kinetic product and the subsequent back transfer of one electron. Studies are continuing to better understand these reactions.

Acknowledgment. We acknowledge the Department of Energy (ER13775) for support of this research and the National Science Foundation (CHE8509862) for an instrument grant to purchase the mass spectrometer.

Trisnorsqualene Alcohol, a Potent Inhibitor of Vertebrate Squalene Epoxidase

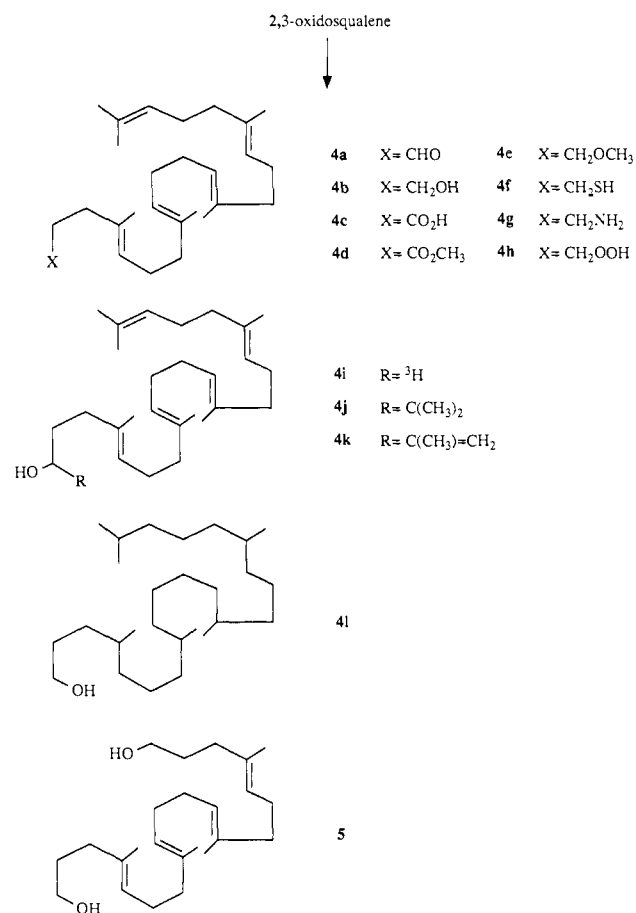
Stephanie E. Sen and Glenn D. Prestwich*

Department of Chemistry
State University of New York
Stony Brook, New York 11794-3400

Received September 12, 1988

The epoxidation of squalene to (3*S*)-2,3-oxidosqualene and its subsequent cyclization to lanosterol are key steps in cholesterol biogenesis.¹ Despite the clinical importance of lowering serum cholesterol levels in humans, no pharmaceuticals are available which specifically target these committed steps in steroidogenesis.² Currently available hypocholesteremic drugs (e.g., mevinolin) inhibit HMG CoA-reductase,³ thus diminishing the supply of mevalonate available for squalene production. Other potential cholesterol-lowering drugs, the oxysterols,⁴ act via a receptor-mediated feedback inhibition of HMG CoA-reductase. Potent in vitro inhibition of oxidosqualene cyclase can be achieved with the aziridyl analogue of oxidosqualene,⁵ as well as with several tertiary amine *N*-oxide transition-state analogues.⁶ However, few compounds which effectively inhibit squalene epoxidase^{7,8} are

Scheme 1^a



^a Trisnorsqualene analogues. **4a**: from 2,3-oxidosqualene (**2**), using H_5IO_6 , THF/ H_2O . **4b**: from **4a**, using NaBH_4 , EtOH. **4c**: from **4a**, using Ag_2O , THF. **4d**: from **4c**, using CH_2N_2 , Et_2O . **4e**: from **4b**, using (1) *n*-BuLi, Et_2O and (2) CH_3I . **4f**: from **4b**, using (1) PPh_3 , DIAD, $\text{CH}_3\text{C}(\text{O})\text{SH}$ and (2) LiAlH_4 , Et_2O . **4g**: from **4b**, using (1) PPh_3 , CBr_4 , CH_2Cl_2 , (2) NaN_3 , DMF, and (3) LiAlH_4 , THF. **4h**: from **4b**, using (1) MsCl , Et_3N , CH_2Cl_2 and (2) H_2O_2 , KOH, MeOH. **4i**: from **4a**, using NaB^3H_4 , EtOH, **4j**: from **4a**, using $(\text{CH}_3)_2\text{CH-MgBr}$, THF. **4k**: from **2**, using LiNEt_2 , THF. **4l**: from **4b**, using H_2 , Pd/C, EtOH. **5**: from hexanorsqualene dialdehyde, using NaBH_4 , EtOH.

Table I. IC_{50} and K_I Values of Squalene Analogues **4a**–**4l** and **5**^a

squalene analogue	IC_{50} (μM)	K_I (μM)	squalene analogue	IC_{50} (μM)	K_I (μM)
4a	200		4h	4	
4b	4	3.5	4i		
4c	>400		4j	>400	
4d	>400		4k	>>400	
4e	300		4l	>>400	
4f	30	13	5	400	
4g	200				

^a Analogues with $\text{IC}_{50} = >400$ showed some inhibition at high [I], while analogues with $\text{IC}_{50} = >>400$ showed essentially no inhibitory effect.

known. Indeed, very little is understood about the enzymatic mechanism of this apparently non-cytochrome P-450-dependent alkene monooxygenase, even in its purified form.⁹ We present

(8) In the course of our work on π -system mimics of the terminal isopropylidene group (Sen, S. E.; Prestwich, G. D., submitted to *J. Med. Chem.*), we found little or no inhibition of the pig liver microsomal epoxidase or cyclase activities by dihaloalkene, allene, acetylene, or cyclopropylidene compounds at maximal concentrations of 400 μM . Recently, the synthesis of several similar compounds and their poor inhibitory activity against rat liver squalene epoxidase was reported: Ceruti, M.; Viola, F.; Grosa, G.; Balliano, G.; Delprino, L.; Cattel, L. *J. Chem. Research (S)* **1988**, 18–19; (*M*) **1988**, 0239–0260.

(1) (a) Mulheirn, L. J.; Ramm, P. J. *Chem. Soc. Rev.* **1972**, 259–291.

(2) Cattel, L.; Ceruti, M.; Viola, F.; Delprino, L.; Balliano, G.; Duriatti, A.; Bouvier-Navé, P. *Lipids* **1986**, *21*, 31–38.

(3) Endo, A. *J. Med. Chem.* **1985**, *28*, 401–410.

(4) (a) Kandutsch, A. A.; Chen, H. W.; Heiniger, H.-J. *Science* **1978**, *201*, 498–501. (b) Parish, E. J.; Nanduri, V. B. B.; Kohl, H. H.; Taylor, F. R. *Lipids* **1986**, *21*, 27–30. (c) Photoaffinity labeling of oxysterol binding protein: Taylor, F. R.; Kandutsch, A. A.; Anzalone, L.; Phirwa, S.; Spencer, T. A. *J. Biol. Chem.* **1988**, *263*, 2264–2269.

(5) Corey, E. J.; Ortiz de Montellano, P. R.; Lia, K.; Dean, P. D. G. *J. Am. Chem. Soc.* **1967**, *89*, 2797–2798. Cell cultures show apparent irreversible inhibition of the cyclase by 2,3-iminosqualene: Popjak, G.; Meenan, A.; Nes, W. D. *Proc. R. Soc. London* **1987**, *B232*, 273–287.

(6) (a) Delprino, L.; Balliano, G.; Cattel, L.; Benveniste, P.; Bouvier, P. *J. Chem. Soc., Chem. Commun.* **1983**, 381–382. (b) Duriatti, A.; Bouvier-Navé, P.; Benveniste, P.; Schuber, F.; Delprino, L.; Balliano, G.; Cattel, L. *Biochem. Pharmacol.* **1985**, *34*, 2765–2777. (c) Ceruti, M.; Balliano, G.; Viola, F.; Cattel, L.; Gerst, N.; Schuber, F. *Eur. J. Med. Chem.* **1987**, *22*, 199–208.

(7) Naftifine (a naphthyl allylamine), terbinafine (a naphthyl enynyl amine) and their congeners inhibit fungal squalene epoxidase: Stütz, A. *Angew. Chem., Int. Ed. Engl.* **1987**, *26*, 320–328. Terbinafine showed K_I values of 0.03 μM for the *Candida albicans* squalene epoxidase and 77 μM for the rat liver enzymes: Ryder, N. S.; Dupont, M.-C. *Biochem. J.* **1985**, *230*, 765–770. In addition, both fungal and rat liver squalene epoxidase are reversibly inhibited by 2-aza-2,3-dihydrosqualene (33 and 2 μM , respectively): Ryder, N. S.; Dupont, M. C.; Frank, I. *FEBS Lett.* **1986**, *204*, 239–242.